

Efficient Visual Transformer by Learnable Token Merging

Yancheng Wang and Yingzhen Yang

Abstract—Self-attention and transformers have been widely used in deep learning. Recent efforts have been devoted to incorporating transformer blocks into different neural architectures, including those with convolutions, leading to various visual transformers for computer vision tasks. In this paper, we propose a novel and compact transformer block, Transformer with Learnable Token Merging (LTM), or LTM-Transformer. LTM-Transformer performs token merging in a learnable scheme. LTM-Transformer is compatible with many popular and compact transformer networks, and it reduces the FLOPs and the inference time of the visual transformers while maintaining or even improving the prediction accuracy. In the experiments, we replace all the transformer blocks in popular visual transformers, including MobileViT, EfficientViT, ViT-S/16, and Swin-T, with LTM-Transformer blocks, leading to LTM-Transformer networks with different backbones. The LTM-Transformer is motivated by reduction of Information Bottleneck, and a novel and separable variational upper bound for the IB loss is derived. The architecture of mask module in our LTM blocks which generate the token merging mask is designed to reduce the derived upper bound for the IB loss. Extensive results on computer vision tasks evidence that LTM-Transformer renders compact and efficient visual transformers with comparable or much better prediction accuracy than the original visual transformers. The code of the LTM-Transformer is available at <https://github.com/Statistical-Deep-Learning/LTM>.

Index Terms—Visual Transformers, Learnable Token Merging, Information Bottleneck, Variational Upper Bound, Compact Transformer Networks

1 INTRODUCTION

BUILDING upon the success of Transformer in natural language processing [1], visual transformers have demonstrated remarkable performance across a wide range of tasks [2], [3], [4], [5], [6], [7]. However, the achievements of visual transformers are accompanied with heavy computational costs [3], [8], making their deployment impractical under resource-limited scenarios. The aforementioned limitations have spurred recent research endeavors aimed at developing efficient visual transformers. In this paper, we study the problem of accelerating visual transformers by token merging.

Token merging is an effective method for reducing the FLOPs and improving the inference speed of visual transformers [9], [10], [11], [12], [13], [14]. However, most existing token merging methods [12], [13], [14], [15] largely sacrifice the prediction accuracy of the original transformer networks for reduced computation costs [14], [16]. These methods [12], [14] generally focus on identifying and merging similar tokens by averaging their features. However, such merging strategies, which are based solely on feature similarity, can potentially diminish the informative features in the tokens that are critical to the prediction tasks. Therefore, it remains an interesting and important question that if we can perform token merging while preserving a compelling performance of the visual transformers after token merging. To this end, we propose a novel transformer block, Transformer with Learnable Token Merging, or LTM-Transformer, which learns how to merge tokens while exhibiting a compelling generalization capability of the transformer with merged tokens.

Motivation. Due to the fact that the FLOPs of a visual transformer largely depend on the number of tokens in all the transformer blocks, the FLOPs of a visual transformer can be significantly reduced by reducing the number of tokens in all the transformer blocks. **Our goal is to merge the output tokens of all the transformer blocks into less tokens without largely sacrificing the prediction accuracy of the original visual transformer.** However, directly merging the output tokens, even by carefully designed methods [12], [13], [14], would adversely affect the performance of the model. In this paper, we propose to maintain a compelling prediction accuracy of a visual transformer with token merging by an informative token merging process. In our LTM-Transformer block, the original attention output tokens of a transformer block are merged into less target tokens, and every target token is an informative weighted average of the original output tokens. All the target tokens, or merged tokens are the final attention output tokens for the LTM-Transformer block, which are fed to an MLP to produce the output of the LTM-Transformer block as illustrated by Figure 1.

Such a token merging process in LTM-Transformer is primarily inspired by the well-known presence of considerable redundancy in the original output tokens of transformer blocks [14], [15]. As different tokens have varying importance in modeling the visual features at a particular transformer block, it is natural to compute an informative aggregation of the original attention output tokens as the final (target) attention output tokens so that more informative and more important tokens contribute more to the merged tokens with a larger weight in the weighted average in the aggregation process.

Such an idea of informative token merging can also be viewed from the perspective of Information Bottleneck (IB). Let Z be the original attention output tokens, which are

• Yancheng Wang and Yingzhen Yang are with School of Computing and Augmented Intelligence, Arizona State University, Tempe, AZ, 85281. E-mail: ywan1053@asu.edu, yingzhen.yang@asu.edu

merged into the merged tokens denoted by \tilde{X} , and let Y be the ground truth training labels for a classification task. \tilde{X} has less tokens than Z . The principle of IB is to maximize the mutual information between \tilde{X} and Y while minimizing the mutual information between \tilde{X} and X . That is, IB encourages the network to learn the merged tokens more correlated with the class labels while reducing their correlation with the input. Extensive empirical and theoretical works have evidenced that models respecting the IB principle enjoy compelling generalization. With the informative token merging process in LTM-Transformer, the merged tokens \tilde{X} are the informative aggregation of the original attention output tokens Z , so \tilde{X} are less correlated with the training images and in this manner the IB principle is better adhered. This is reflected in Table 5 in Section 4.4, where a model for ablation study with token merging, ToMe, enjoys less IB loss than the vanilla transformer, MobileViT-S. This observation indicates that the IB principle is better respected by the token merging process in ToMe. In order to further decrease the IB loss, we propose an Information Bottleneck (IB) inspired token merging process, where a LTM-Transformer block generates an informative token merging task which reduces the IB loss for visual transformers. For example, our model termed ‘‘LTM-MobileViT-S’’ in Table 5 is the visual transformer with the IB loss reduced by replacing all the transformer blocks in MobileViT-S with LTM-Transformer blocks so that more informative merged tokens are generated by the proposed informative token merging process. While ToMe hurts the prediction accuracy compared to the vanilla model, our LTM-Transformer enjoys even higher top-1 accuracy than the vanilla MobileViT-S, and we have the same observations for MobileViT-XS and EfficientViT.

1.1 Contributions

The contributions of this paper are presented as follows.

First, we present a novel and compact transformer block termed Transformer with Learnable Token Merging, or LTM-Transformer. Our LTM-Transformer block generates an informative token merging mask which reduces the IB loss. The LTM-Transformer blocks can be used to replace all the transformer blocks in many popular visual transformers, rendering compact visual transformers with competitive performance. The effectiveness of LTM-Transformer is evidenced by replacing all the transformer blocks in popular visual transformers which are already compact, including MobileViT [17], EfficientViT [7], ViT-S/16 [3], and Swin-T [4], with LTM-Transformer blocks, for image classification, object detection and instance segmentation tasks.

Second, we propose an informative token merging process for visual transformers which can reduce the IB loss. As a first step, we derive a novel and *separable* variational upper bound for the IB loss associated with token merging, which is $I(\tilde{X}(G)) - I(\tilde{X}(G), Y)$ where $I(\cdot, \cdot)$ denotes mutual information and G is the token merging mask in LTM-Transformer. We then view a transformer with multiple LTM-Transformer blocks as an iterative process for reduction of the IB loss by gradient descent, and every LTM-Transformer block performs one-step gradient descent on the variational upper bound for the IB loss. Inspired by this understanding,

the token merging mask at the current layer is generated from the token merging mask at the previous layer and the input tokens at the current layer by a learnable mask module, following the formula of gradient descent as in (3) in Section 3.2. As a result, such informative token merging process generates in a network with LTM-Transformer blocks enjoys reduced IB loss, which is evidenced in our ablation study in Section 4.4. Due to the separability of the variational upper bound for the IB loss, a neural network with LTM-Transformer blocks can be trained in an end-to-end manner with standard SGD. We remark that as shown in Table 5, a baseline token merging method, ToMe, can already reduce the IB loss. By replacing all the transformer blocks with our LTM-Transformer blocks, the network with LTM-Transformer enjoys smaller IB loss, higher classification accuracy and less FLOPs. Importantly, extensive experiment results on various computer vision tasks demonstrate the compelling performance of LTM-Transformer networks compared to the competing baselines.

It is worthwhile to mention that our LTM-Transformers are trained from scratch, while most existing token merging methods [12], [13], [14] perform token merging on a trained transformer without additional training [14] or with a light training process [12], [13]. The training time of LTM-Transformers with comparison to competing token merging methods is presented in Table 6 of Section 5.1.

This paper is organized as follows. The related works in efficient visual transformers and compression of visual transformers by pruning or token merging are discussed in Section 2. The formulation of LTM-Transformer is detailed in Section 3. The effectiveness of LTM-Transformer is demonstrated in Section 4 for image classification, object detection and instance segmentation tasks, by replacing all the transformer blocks of various popular visual transformers, including MobileViT [17], EfficientViT [7], ViT-S/16 [3], and Swin-T [4], with LTM-Transformer blocks. Our ablation studies are presented in Section 5 and Section 4.4, and the proofs of theoretical results are in Section 6. We conclude the paper in Section 7. Throughout this paper we use $[n]$ to denote the natural numbers between 1 and n inclusively.

2 RELATED WORKS

2.1 Efficient Visual Transformers

Visual transformer models have recently achieved superior performance on a variety of computer vision applications [4], [5], [6], [18], [19], [20]. However, visual transformers often encounter high computational demands due to the quadratic complexity of the point-wise attention and numerous Multi-Layer Perceptron (MLP) layers. To mitigate the challenges of high computational costs, various strategies have been developed [2], [5], primarily aimed at refining the network architectures and incorporating sparse mechanisms for efficient computation. These include the integration of convolutions into transformer networks [7], [17], [21], the use of knowledge distillation for training more efficient transformers [22], [23], [24], and compressing existing visual transformers with methods such as pruning [25], [26], [27]. Techniques for compressing visual transformers generally fall into three categories: (1) Channel Pruning, which targets the elimination of superfluous heads and channels within

ViT blocks [25], [28], [29]; (2) Block Pruning, which involves removing redundant transformer blocks [26], [30]; (3) Token Pruning and Token Merging, which prune less important tokens and merge similar tokens in the input of transformer blocks [14], [15], [27], [31].

In this paper, we focus on learning to merge tokens guided by the information bottleneck theory of deep learning and primarily review existing works on Token Pruning and Merging [12], [13], [14], [15], [31]. DynamicViT [15] observes that the prediction in visual transformers is only based on a subset of the most informative tokens and proposes a hierarchical token sparsification framework to prune redundant tokens. ToMe [14] proposes a graph-based matching algorithm that combines similar tokens in each visual transformer block of a pre-trained visual transformer. LTMP [13] learns threshold masking modules that dynamically determine which tokens to merge and prune in a unified framework similar to DynamicViT. ToFu [12] also combines token pruning and token merging. Instead of average merging similar tokens, ToFu proposes a conventional average merging module to improve the quality of merged tokens.

2.2 Related Works about Information Bottleneck

[32] provides the first in-depth analysis of conventional information bottleneck (IB) theories and deep learning to establish the connection between the nonlinearity of neural networks and the compression phase of training. Building on the theory of IB, [33] proposes a probabilistic attention module reducing mutual information between the input and the masked representation while increasing mutual information between the masked representation and the task label. Further exploring the mechanics of IB in deep learning, [34] finds that self-attention mechanisms can be interpreted as iterative steps in optimizing the IB objective, which explains the advantages of self-attention in learning robust representation. Distinct from most existing methods that implicitly incorporate the IB principle, our work adopts a direct and innovative approach. We aim to optimize a novel and separable variational upper bound of the IB loss with a learnable token merging method. The proposed LTM-Transformer lead to compelling performance on many popular visual transformer architecture with lower computation cost, benefiting from the learnable token merging mechanism guided by the IB principle.

3 FORMULATION

In this section, we first illustrate how to perform token merging using a token merging mask. We then describe how to generate the token merging mask from a learnable mask module in a LTM-Transformer block, as well as the training algorithm of a neural network with LTM-Transformer blocks. We derive a novel and separable variational upper bound for the IB loss, and the token merging masks are generated to reduce such variational upper bound for the IB loss.

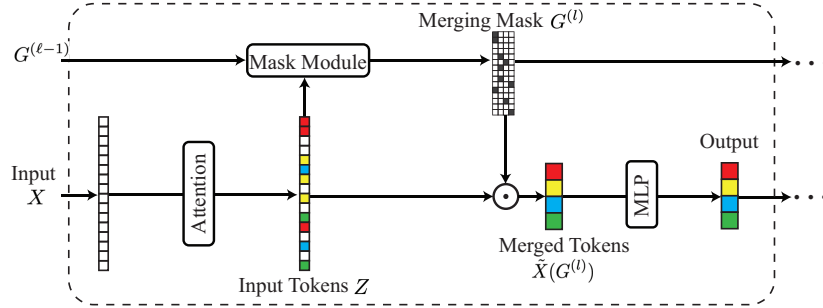
3.1 Token Merging by Learnable Token Merging Masks

Given the input feature tokens $X \in \mathbb{R}^{N \times D}$ where N is the number of tokens and D is the token dimension, the LTM-Transformer block first applies the self-attention module on

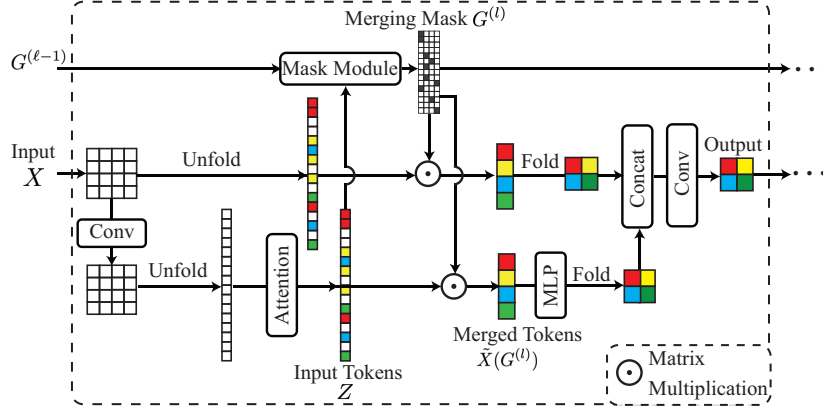
the input feature tokens by $Z = \text{ATTN}(X)$, where $\text{ATTN}(\cdot)$ is the regular QKV self-attention operation [35]. As illustrated in Figure 1, every LTM-Transformer block has an MLP as a learnable mask module which generates the token merging mask $G^{(\ell)}$ where ℓ is the index of the current layer or block. The LTM-Transformer block merges the N tokens of Z into P tokens with $P < N$ by multiplying Z with the token merging mask $G^{(\ell)} \in \mathbb{R}^{N \times P}$. We set $P = \lceil r \times N \rceil$, where $r \in (0, 1)$ is termed the compression ratio for LTM, and a smaller r renders less merged tokens after token merging. The token merging mask $G^{(\ell)}$ of the ℓ -th transformer block is generated by the token merging mask $G^{(\ell-1)}$ of the previous layer and the feature tokens Z , which is motivated by reducing the IB loss and detailed in Section 3.2. The token merging mask $G^{(1)}$ for the first block is generated from the input feature tokens of the first layers by $G^{(1)} = \text{Softmax}(f(X/\tau))$, where $f(\cdot)$ represents an MLP layer followed by a Sigmoid function. $\tau \in (0, 1)$ is a temperature parameter that aims to sparsify the merging mask. After obtaining the merging mask $G^{(\ell)}$, the features tokens of Z are merged into P tokens by $\tilde{X}(G^{(\ell)}) = (Z^\top G^{(\ell)})^\top \in \mathbb{R}^{P \times D}$, which is then passed to the following MLP layers in the transformer block.

In addition to merging tokens in regular transformer blocks such as ViT [35] and Swin [4], the LTM-Transformer block can also be applied to efficient transformer blocks widely applied in efficient visual transformer architectures such as MobileViT [17] and EfficientViT [7]. Regular transformer blocks obtain the output by sequentially applying the attention operation and MLP on the input feature tokens. However, efficient transformer blocks usually contain residual connections following the design of residual connections in Convolutional Neural Networks (CNNs). That is, these blocks maintain the same shapes for the input X and the self-attention output Z and concatenate them to produce the output features of the current transformer block. As a result, we cannot only merge the tokens of Z . Instead, our LTM-Transformer block merges the tokens of both X and Z so that the number of merged tokens for X and Z have is the same. To this end, we apply the same token merging mask $G^{(\ell)}$ to merge both X and Z . As a result, the compressed X and Z are of the same shape after the token merging process and they can still be concatenated, which is illustrated in Figure 1(b). In addition, transformer blocks in the efficient visual transformers are usually accompanied with convolution operations so that they need to maintain the feature tokens in a three-dimensional format $X \in \mathbb{R}^{H \times W \times D}$ as illustrated in Figure 1(b). To apply our token merging method on efficient transformer blocks, we set the number of merged tokens after token merging as $P = H' \times W'$, where r is the compression ratio, and $H' = \lceil H \times \sqrt{r} \rceil$, $W' = \lceil W \times \sqrt{r} \rceil$. Therefore, the merged tokens can still be reshaped into three-dimensional features for later convolution operations. The analysis about the inference computation cost, or the FLOPs, of the LTM transformer block for token merging in both regular transformers and efficient transformers as illustrated in Figure 1 is detailed below.

Computation Cost Analysis of LTM-Transformer for Token Merging. We hereby analyze the additional inference computation cost, or the FLOPs, of the LTM transformer block for token merging in both regular transformers and



(a) LTM-Transformer block for regular transformers, such as ViT and Swin.



(b) LTM-Transformer block for efficient transformers, such as MobileViT and EfficientViT.

Fig. 1: Overall framework of Learnable Token Merging (LTM)-Transformer block for regular transformer blocks such as ViT and Swin (a), and efficient transformer blocks such as MobileViT and EfficientViT (b).

efficient transformers as illustrated in Figure 1. Let D be the dimension of input tokens and N be the number of tokens. The FLOPs of the token merging in an LTM transformer block in regular visual transformers is $6CDP + 3C + ND^2 + NDP$, where $6CDP + 3C + ND^2$ is the FLOPs for calculating the merging mask and NDP is the cost for applying the merging mask on the input tokens. In the LTM transformer block of efficient visual transformers, the additional FLOPs of the token merging is $6CDP + 3C + ND^2 + 2NDP$, since the merging mask will be applied to both the input tokens and the merged tokens.

3.2 Generating Token Merging Mask by Reducing Variational Upper Bound for the IB Loss

We describe how to generate the token merging mask in a LTM-Transformer block in this subsection, and the generation of the token merging mask is inspired by reduction of the IB loss. We first introduce the setup where the IB loss can be specified.

Given the training data $\{X_i, y_i\}_{i=1}^n$ where X_i is the i -th input training feature and y_i is the corresponding class label. Let Z_i be the self-attention output tokens of the X_i , and $\tilde{X}_i(G) = (Z_i G)^T$ is the merged tokens with G being the token merging mask. We first specify how to compute the IB loss, $\text{IB}(G) = I(\tilde{X}(G), X) - I(\tilde{X}(G), Y)$ which depends on G and other network parameters, X is a random variable representing the input feature which takes values in $\{X_i\}_{i=1}^n$, $\tilde{X}(G)$ is a random variable representing the merged tokens

which takes values in $\{\tilde{X}_i(G)\}_{i=1}^n$. Y is a random variable representing the class label which takes values in $\{y_i\}_{i=1}^n$. After performing K-means clustering on $\{\tilde{X}_i(G)\}_{i=1}^n$ and $\{X_i\}_{i=1}^n$, we have the clusters $\{\tilde{C}_a\}_{a=1}^C$ and $\{C_b\}_{b=1}^C$ for the merged tokens and the input features respectively, where C is the number of classes. We also abbreviate $\tilde{X}(G)$ as \tilde{X} for simplicity of the notations. Then we define the probability that \tilde{X} belongs to cluster \tilde{C}_a as $\Pr[\tilde{X} \in a] = \frac{1}{n} \sum_{i=1}^n \phi(\tilde{X}_i, a)$

with $\phi(\tilde{X}_i, a) = \frac{\exp(-\|\tilde{X}_i - \tilde{C}_a\|_2^2)}{\sum_{a=1}^C \exp(-\|\tilde{X}_i - \tilde{C}_a\|_2^2)}$. Similarly, we define the probability that X_i belongs to cluster C_b as $\Pr[X \in b] = \frac{1}{n} \sum_{i=1}^n \phi(X_i, b)$. Moreover, we have the joint probabilities $\Pr[\tilde{X} \in a, X \in b] = \frac{1}{n} \sum_{i=1}^n \phi(\tilde{X}_i, a) \phi(X_i, b)$

and $\Pr[\tilde{X} \in a, Y = y] = \frac{1}{n} \sum_{i=1}^n \phi(\tilde{X}_i, a) \mathbb{I}_{\{y_i=y\}}$ where $\mathbb{I}_{\{ \cdot \}}$ is an indicator function. As a result, we can compute the mutual information $I(\tilde{X}(G), X)$ and $I(\tilde{X}(G), Y)$ by

$$I(\tilde{X}(G), X) = \sum_{a=1}^C \sum_{b=1}^C \Pr[\tilde{X}(G) \in a, X \in b] \log \frac{\Pr[\tilde{X}(G) \in a, X \in b]}{\Pr[\tilde{X}(G) \in a] \Pr[X \in b]},$$

$$I(\tilde{X}(G), Y) = \sum_{a=1}^C \sum_{y=1}^C \Pr[\tilde{X}(G) \in a, Y = y] \log \frac{\Pr[\tilde{X} \in a, Y = y]}{\Pr[\tilde{X}(G) \in a] \Pr[Y = y]},$$

and then compute the IB loss $\text{IB}(G)$. As explained in

our motivation, we aim to perform token merging while can reduce the IB loss. However, directly optimizing the IB loss in the standard SGD training is difficult as the IB loss is not separable. Given a variational distribution $Q(\tilde{X} \in a|Y = y)$ for $y, a \in [C]$ computed by Eq. (8) in Section 6.3, the following theorem gives a variational upper bound, $\text{IBB}(G)$, for the IB loss $\text{IB}(G)$. $\text{IBB}(G)$ is separable and thus compatible with SGD training with minibatches.

Theorem 3.1.

$$\text{IB}(G) \leq \text{IBB}(G) - C_0, \quad (1)$$

where C_0 is a constant only depending on the input training features $\{X_i\}_{i=1}^n$, and

$$\begin{aligned} \text{IBB}(G) := & \frac{1}{n} \sum_{i=1}^n \sum_{a=1}^C \sum_{b=1}^C \phi(\tilde{X}_i(G), a) \phi(X_i, b) \log \phi(X_i, b) \\ & - \frac{1}{n} \sum_{i=1}^n \sum_{a=1}^C \sum_{y=1}^C \phi(\tilde{X}_i(G), a) \mathbb{I}_{\{y_i=y\}} \log Q(\tilde{X} \in a|Y = y). \end{aligned}$$

Proposition 3.2. Suppose $\tilde{X}_i(G) = (Z_i^\top G)^\top \in \mathbb{R}^{P \times D}$ with $Z_i \in \mathbb{R}^{N \times D}$ being the self-attention output tokens for the i -th training feature and $G \in \mathbb{R}^{N \times P}$ is the token merging mask where N is the number of tokens, D is the token dimension, P is the number of merged tokens after token merging, and $\tilde{X}_i(G)$ denotes the merged tokens. At step ℓ of gradient descent on $\text{IBB}(G)$, we have

$$\begin{aligned} G^{(\ell)} &= G^{(\ell-1)} - \eta \nabla_G \text{IBB}(G^{(\ell-1)}) \\ &= G^{(\ell-1)} - \frac{2\eta}{n} \sum_{i=1}^n \sum_{a=1}^C Z_i \frac{S_{ia}^{(\ell-1)}}{(\gamma_i^{(\ell-1)})^2} \left(\gamma_i^{(\ell-1)} \mathcal{C}_a - \zeta_i^{(\ell-1)} \right) \psi_{i,a}, \quad \ell \geq 2, \end{aligned} \quad (2)$$

where $S_{ia}^{(\ell)} := \exp\left(-\left\|\tilde{X}_i(G^{(\ell)}) - \tilde{\mathcal{C}}_a\right\|_2^2\right)$ for $i \in [n]$ and $a \in [C]$, $\gamma_i^{(\ell)} := \sum_{a=1}^C S_{ia}^{(\ell)}$, $\zeta_i^{(\ell)} := \sum_{a=1}^C S_{ia}^{(\ell)} \tilde{\mathcal{C}}_a$ for $i \in [n]$, $\psi_{i,a} := \sum_{b=1}^C \phi(X_i, b) \log \phi(X_i, b) - \sum_{y=1}^C \mathbb{I}_{\{y_i=y\}} \log Q(\tilde{X} \in a|Y = y)$.

The proofs of Theorem 3.1 and Proposition 3.2 are deferred to Section 6. Inspired by Proposition 3.2, we can understand a transformer with token merging and multiple transformer blocks as an iterative process which reduces $\text{IBB}(G)$ by gradient descent, where the ℓ -th transformer block performs one-step gradient descent on $\text{IBB}(G)$ according to (2). The mask module of at the ℓ -th LTM-Transformer block generates the token merging mask $G^{(\ell)}$ from $G^{(\ell-1)}$, the token merging mask of the previous block, through (2). To improve the flexibility of the token merging mask, an MLP is applied on Z_i . Moreover, as IBB and $\nabla_G \text{IBB}$ are separable, (2) can be performed on a minibatch $\mathcal{B}_j \subseteq \{1, \dots, n\}$, which is compatible with minibatch-based training with SGD for a transformer network with LTM-Transformer blocks. That is, the mask module of the ℓ -th LTM-Transformer block generates $G^{(\ell)}$ by

$$\begin{aligned} G^{(\ell)} &= G^{(\ell-1)} \\ & - \frac{2\eta}{n} \sum_{i \in \mathcal{B}_j} \sum_{a=1}^C \text{MLP}(Z_i) \frac{S_{ia}^{(\ell-1)}}{(\gamma_i^{(\ell-1)})^2} \left(\gamma_i^{(\ell-1)} \mathcal{C}_a - \zeta_i^{(\ell-1)} \right) \psi_{i,a}, \end{aligned} \quad (3)$$

where $\text{MLP}(\cdot)$ consists of two linear layers of the same hidden dimension with a ReLU activation in the middle, and each LTM-Transformer block has its own MLP.

Algorithm 1 Training Algorithm of LTM-Transformers

- 1: Initialize the weights of the network by $\mathcal{W} = \mathcal{W}(0)$ through random initialization, set t_{train} which is the number of training epochs.
 - 2: **for** $t \leftarrow 1$ to t_{train} **do**
 - 3: **if** $t < t_{\text{warm}}$ **then**
 - 4: Perform gradient descent by a standard step of SGD without applying token merging in LTM transformer blocks.
 - 5: **else**
 - 6: Update $\phi(\tilde{X}_i, a)$ for all the clusters $a \in [C]$ and $i \in [n]$.
 - 7: **for** $j \leftarrow 1$ to J **do**
 - 8: **Forward step:** generate $\{G^{(\ell)}\}$ for all the LTM-Transformer blocks by (3) using the minibatch \mathcal{B}_j , the updated $\{\phi(\tilde{X}_i, a)\}_{i \in \mathcal{B}_j, a \in [C]}$, $\{Q^{(t-1)}(\tilde{X} \in a|Y = y)\}_{a \in [C], y \in [C]}$ and $\{\tilde{\mathcal{C}}_a^{(t-1)}\}_{a=1}^C$, as well as the output of the network
 - 9: **Backward step:** update the MLP layers of the mask modules in all the LTM-Transformer blocks as well as all the other weights in the neural network by a standard step of SGD on the cross-entropy loss
 - 10: **end for**
 - 11: Compute $Q^{(t)}(\tilde{X} \in a|Y = y)$ by Eq. (8) in Section 6.3, perform K-means clustering on $\{\tilde{X}_i\}_{i=1}^n$ and update the clusters $\{\tilde{\mathcal{C}}_a^{(t)}\}_{a=1}^C$.
 - 12: **end if**
 - 13: **end for**
 - 14: **return** The trained weights \mathcal{W} of the network
-

Algorithm 1 describes the training process of a neural network with LTM-Transformer blocks using the standard cross-entropy loss for a classification problem. It is remarked that all the MLP layers of the mask modules in all the LTM-Transformer blocks, along with other network parameters, are updated with standard SGD. In order to generate the token merging masks for all the LTM-Transformer blocks before a new epoch starts, we update the variational distribution $Q^{(t)}$ and the clusters $\{\tilde{\mathcal{C}}_a^{(t)}\}_{a=1}^C$ at the end of the previous epoch.

4 EXPERIMENTAL RESULTS

In this section, LTM-Transformers are assessed for the image classification task on the ImageNet-1k dataset. The results in Section 4.1 indicate that LTM outperforms existing state-of-the-art networks while maintaining a more compact architecture. In addition, LTM is compared with existing methods on token merging and shows better performance with lower computation costs. Furthermore, in Sections 4.2 and 4.3, we demonstrate that the use of LTM-MobileViT and LTM-EfficientViT as feature extraction backbones leads to superior mAP and reduced FLOPs compared to the baseline models for the tasks of object detection and semantic segmentation. In Section 4.4, we perform ablation studies on the effects of LTM-Transformer in reducing the IB loss and the IB bound at different layers of a LTM-Transformer network.

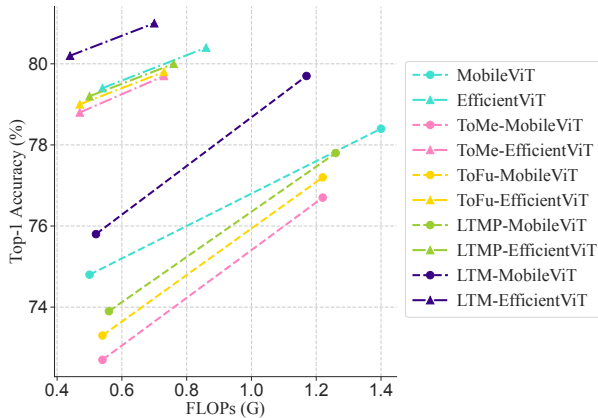


Fig. 2: Top-1 accuracy vs FLOPs (G) on ImageNet-1k validation set.

4.1 Image Classification

Implementation details. ImageNet [36] classification, we employ MobileViT-S [17], MobileViT-XS [17], EfficientViT-B1 [7], ViT-S [35], and Swin-T [4] as backbone architectures. We substitute the conventional transformer blocks in these backbones with LTM-Transformer blocks. During the training of LTM-Transformers, we utilize the AdamW optimizer with $\beta_1 = 0.9$ and $\beta_2 = 0.999$. The training process spans 300 epochs, starting with a warm-up phase during which token merging is not applied in all the LTM-transformer blocks. After the warm-up stage, we enable token merging in all the LTM-transformer blocks. t_{warm} is fixed to 100 in all the experiments. All the experiments are conducted on four NVIDIA A100 GPUs with a total batch size of 1024 images. Following prior works [4], our training incorporates popular data augmentation methods such as RandAugment, Mixup, Cutmix, and random erasing. We set the weight decay at 0.01. The learning rate initially increases from 0.0002 to 0.002 over the first 10 epochs and is subsequently reduced back to 0.0002 following a cosine decay schedule. We set η in (2) to 1 in all the experiments. In addition, we apply a softmax operation on the token merging mask at each layer to ensure the aggregation weights for each merged tokens sum to 1.

Results. As shown in Table 1, models integrated with LTM-Transformer blocks show reduced FLOPs and enhanced accuracy compared to their original visual transformer counterparts, at a cost of very slight increase of model size due to the extra parameters in the mask modules of the LTM-Transformer blocks. For instance, LTM-MobileViT-S not only reduces its FLOPs from 1.4G to 1.17G but also improves accuracy by 1.3% over the original MobileViT-S, with a slight increase of the model size by 0.3M. Similarly, LTM-MobileViT-XS achieves a 1.0% accuracy increase while lowering its FLOPs from 0.7G to 0.52G compared to the original model, with a slight increase of model size by 0.2M. To further demonstrate the efficiency of the LTM-Transformer, we compare it against current state-of-the-art weight pruning methods for efficient visual transformers, including S²ViTE [38], SPViT [39], and SAViT [40] on EfficientViT-B1 (r224). To apply S²ViTE, SPViT, and SAViT on EfficientViT-B1 (r224), we first run their pruning process following the standard implementation in their papers [38], [39], [40] on the

Model	# Params	FLOPs	Top-1
MobileViT-XS	2.3 M	0.7 G	74.8
ToMe-MobileViT-XS [14]	2.3 M	0.54 G	72.7
ToFu-MobileViT-XS [12]	2.3 M	0.54 G	73.3
LTMP-MobileViT-XS [13]	2.3 M	0.56 G	73.9
LTM-MobileViT-XS (Ours)	2.5 M	0.52 G	75.8
MobileFormer	9.4 M	0.2 G	76.7
EfficientFormer [37]	12.3 M	1.3 G	79.2
MobileViT-S	5.6 M	1.4 G	78.4
ToMe-MobileViT-S [14]	5.6 M	1.22 G	76.7
ToFu-MobileViT-S [12]	5.6 M	1.22 G	77.2
LTMP-MobileViT-S [13]	5.6 M	1.26 G	77.5
LTM-MobileViT-S (Ours)	5.9 M	1.17 G	79.7
EfficientViT-B1 [r224] [7]	9.1 M	0.52 G	79.4
S ² ViTE-EfficientViT-B1 [r224] [38]	8.2 M	0.47 G	79.0
SPViT-EfficientViT-B1 [r224] [39]	9.2 M	0.49 G	79.3
SAViT-EfficientViT-B1 [r224] [40]	8.4 M	0.47 G	79.2
ToMe-EfficientViT-B1 [r224] [14]	9.1 M	0.47 G	78.8
ToFu-EfficientViT-B1 [r224] [12]	9.1 M	0.47 G	79.0
LTMP-EfficientViT-B1 [r224] [13]	9.1 M	0.50 G	79.2
LTM-EfficientViT-B1 [r224] (Ours)	9.5 M	0.44 G	80.2
EfficientViT-B1 [r288] [7]	9.1 M	0.86 G	80.4
ToMe-EfficientViT-B1 [r288] [14]	9.1 M	0.73 G	79.7
ToFu-EfficientViT-B1 [r288] [12]	9.1 M	0.73 G	79.8
LTMP-EfficientViT-B1 [r288] [13]	9.1 M	0.76 G	80.0
LTM-EfficientViT-B1 [r288] (Ours)	9.5 M	0.70 G	81.0
ViT-S/16 [3]	22.1 M	4.3 G	81.2
LTM-ViT-S/16 (Ours)	23.0 M	3.7 G	81.8
Swin-T [4]	29.0 M	4.5 G	81.3
LTM-Swin-T (Ours)	30.5 M	3.8 G	81.8

TABLE 1: Comparisons with baseline methods on ImageNet-1k validation set.

ImageNet training data. After obtaining the pruned networks, we fine-tune them using the same setting as in [7]. As LTM-Transformer focuses on token merging, we compare our LTM-Transformer models with existing token merging methods, including ToMe [14], ToFu [12], and LTMP [13]. All the token merging methods, ToMe [14], ToFu [12], LTMP [13], and our LTM-Transformer, are applied on the same visual transformer backbone. It is observed from Table 1 that with even lower FLOPs, LTM-Transformer models consistently outperform the competing token merging methods.

In addition, we apply LTM-Transformer to ViT-B with two different FLOPs budgets and compare LTM-Transformer with ViT-B models accelerated by ToMe, ToFu, and LTMP in Table 2. The inference time of all the models are also evaluated on the validation set of ImageNet-1k and reported in milliseconds (ms) per batch for an evaluation batch size of 128 on one Nvidia A100 GPU. It is observed that LTM-Transformer models outperform the competing token merging methods with even lower FLOPs and faster inference speed. Remarkably, LTM-ViT-B with 12.85G FLOPs has even higher top-1 accuracy than the vanilla ViT-B, evidencing the effectiveness of the informative token merging process in LTM-Transformer blocks.

4.2 Object Detection

Implementation details. We incorporate ImageNet pre-trained models, that are LTM-MobileViT-XS, LTM-MobileViT-

Methods	# Params.	FLOPs	Inference Time (ms/batch)	Top-1
ViT-B	86.5 M	17.58 G	37.2	83.74
ViT-B (ToMe [14])	86.5 M	8.78 G	25.4	78.88
ViT-B (ToFu [12])	86.5 M	8.78 G	26.0	80.70
ViT-B (LTMP [13])	86.5 M	8.84 G	27.1	81.21
LTM-ViT-B	90.0 M	8.30 G	25.2	82.23
ViT-B (ToMe [14])	86.5 M	13.12 G	31.0	82.86
ViT-B (ToFu [12])	86.5 M	13.12 G	31.5	83.22
ViT-B (LTMP [13])	86.5 M	13.46 G	32.7	83.29
LTM-ViT-B	90.4 M	12.85 G	30.7	83.87

TABLE 2: Performance comparison with token pruning methods on ImageNet.

S, and LTM-EfficientViT, with the single-shot object detection backbone, SSDLite [41], to evaluate on the MS-COCO dataset [42], which comprises 117k training images and 5k validation images. We fine-tune all pre-trained LTM-Transformers within the object detection framework at a standard input resolution of 320×320 . These models undergo a training period of 200 epochs using the AdamW optimizer, adhering to the training protocols established in [17]. Employing a cosine learning rate scheduler, the initial learning rate of 0.0009 is gradually reduced to $1.6e^{-6}$. For the object localization, we utilize a smooth ℓ^1 loss, and for classification, cross-entropy losses are applied. The evaluation of performance on the validation set is conducted using the mAP metric with an IoU range from 0.50 to 0.95 in increments of 0.05.

Feature backbone	# Params.	FLOPs	mAP
MobileNetv3 [43]	4.9 M	1.4 G	22.0
MobileNetv2 [41]	4.3 M	1.6 G	22.1
MobileNetv1 [44]	5.1 M	2.6 G	22.2
MixNet [45]	4.5 M	2.2 G	22.3
MNASNet [46]	4.9 M	1.7 G	23.0
YoloV5-N (640×640) [47]	1.9 M	4.5 G	28.0
VidT [48]	7.0 M	6.7 G	28.7
MobileViT-XS	2.7 M	1.7 G	24.8
LTM-MobileViT-XS(Ours)	2.9 M	1.5 G	25.4
MobileViT-S	5.7 M	2.4 G	27.7
LTM-MobileViT-S(Ours)	6.0 M	2.1 G	28.4
EfficientViT	9.9 M	1.5 G	28.4
LTM-EfficientViT(Ours)	10.3 M	1.4 G	28.9

TABLE 3: Object detection performance with SSDLite.

Results. We adopt a comparative study of our LTM Transformers against other lightweight feature backbones within the SSDLite object detection framework. The results, as detailed in Table 3, illustrate significant improvements in object detection performance when the feature backbone is upgraded to include LTM-Transformer blocks. For example, substituting MobileViT-S with LTM-MobileViT-S enhances the mAP by 0.7% while concurrently reducing FLOPs by 0.3G. Additionally, SSDLite equipped with LTM-EfficientViT achieves a substantial performance increase of 6.9% while maintaining the same FLOPs as MobileNetV3.

4.3 Instance Segmentation

In this section, we assess the efficacy of LTM when applied to instance segmentation tasks using the COCO dataset [42]. We utilize Mask R-CNN [49] equipped with a Feature Pyramid

Network (FPN) as the segmentation head, built on the LTM-EfficientViT-B1 feature backbone. For comparative analysis, we include EfficientViT-B1 [7] and EViT [21] as baseline models. Both our models and the baselines are trained on the training split of the COCO dataset and evaluated on the validation split, adhering to the protocols established by [50]. The training duration is set to 12 epochs, consistent with the $1 \times$ schedule described in [50]. The AdamW optimizer is employed for training following the practices of [21]. We initiate the learning rate at 0.001, which is then gradually reduced following a cosine learning rate schedule. Performance metrics reported include the mean bounding box Average Precision (mAP^b) and mean mask Average Precision (mAP^m), along with bounding box Average Precision (AP^b) and mask Average Precision (AP^m) at IoU thresholds of 0.5 and 0.75. The findings, detailed in Table 4, demonstrate that LTM-EfficientViT-B1 consistently enhances segmentation performance across various thresholds.

Methods	mAP^{box}	$AP_{0.5}^b$	$AP_{0.75}^b$	mAP^m	$AP_{0.5}^m$	$AP_{0.75}^m$
EViT [21]	32.8	54.4	34.5	31.0	51.2	32.2
EfficientViT-B1 [7]	33.5	55.4	34.8	31.9	52.3	32.7
LTM-EfficientViT-B1	34.3	56.1	35.2	32.8	52.8	33.1

TABLE 4: Instance Segmentation Results on COCO.

4.4 Ablation Study

Study on the effects of LTM in reducing IB loss. We study the effectiveness of LTM-Transformer in reducing the IB loss and the variational upper bound of IB loss, which is the IB bound, across three visual transformers, including MobileViT-S, MobileViT-XS, and EfficientViT (r224). We compare the performance of the visual transformers with the baseline token merging method, ToMe [14], and the corresponding LTM-Transformer models with all the transformer blocks replaced with the LTM-Transformer blocks. The results are shown in Table 5. The results indicate that although ToMe reduces the IB loss and the IB bound, thereby adhering to the IB principle which aims to enhance the correlation of features with class labels while reducing their correlation with the input, LTM can further decrease the IB loss and IB bound. In particular, our LTM-Transformer models improve the vanilla visual transformers and the ToMe models by a large margin in terms of both IB loss and top-1 accuracy.

Model	# Params	FLOPs	Top-1	IB Bound	IB Loss
MobileViT-S	5.6 M	1.40 G	78.4	0.05782	-0.00432
ToMe-MobileViT-S	5.6 M	1.22 G	76.7	0.04542	-0.00913
LTM-MobileViT-S	5.9 M	1.17 G	79.7	0.02791	-0.01773
MobileViT-XS	2.3 M	0.71 G	74.8	0.05539	-0.00419
ToMe-MobileViT-XS	2.3 M	0.54 G	72.7	0.04583	-0.00647
LTM-MobileViT-XS	2.5 M	0.52 G	75.8	0.03082	-0.01618
EfficientViT (r224)	9.1 M	0.52 G	79.4	0.06014	-0.00451
ToMe-EfficientViT (r224)	9.1 M	0.47 G	78.8	0.04642	-0.00732
LTM-EfficientViT (r224)	9.5 M	0.44 G	80.2	0.02886	-0.01539

TABLE 5: Ablation Study on the effects of LTM in reducing IB loss.

Study on the IB loss and IB bound at different layers.

To study how the IB loss $IB(G)$, and the variational upper bound for the IB loss, $IBB(G)$, decrease with respect to layer index ℓ of a LTM-Transformer network, $IB(G)$ and $IBB(G)$

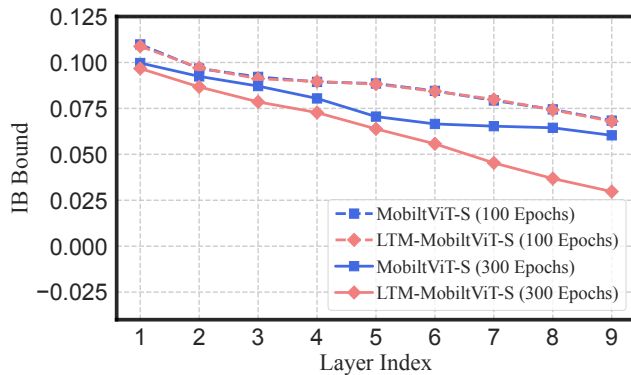
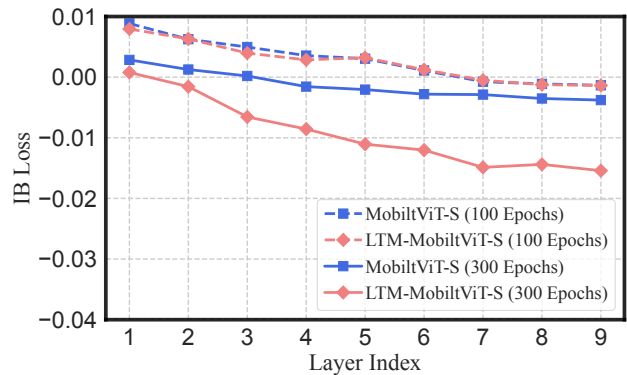
(a) IB bound ($IBB(G)$) comparison between MobileViT-S and LTM-MobileViT-S.(b) IB loss ($IB(G)$) comparison between MobileViT-S and LTM-MobileViT-S.

Fig. 3: IB bound and IB loss comparison between MobileViT-S and LTM-MobileViT-S at different transformer layers.

Methods	# Params	FLOPs	Training Time (Hours)	Top-1
MobileViT-XS	2.3 M	0.70 G	73.5	75.8
ToMe-MobileViT-XS	2.3 M	0.54 G	73.5	72.7
ToFu-MobileViT-XS	2.3 M	0.54 G	73.5	73.3
LTMP-MobileViT-XS	2.3 M	0.56 G	73.8	73.9
LTM-MobileViT-XS	2.5 M	0.52 G	91.0	76.8
MobileViT-S	5.6 M	1.40 G	89.5	78.4
ToMe-MobileViT-S	5.6 M	1.22 G	89.5	76.7
ToFu-MobileViT-S	5.6 M	1.22 G	89.5	77.2
LTMP-MobileViT-S	5.6 M	1.17 G	90.0	77.5
LTM-MobileViT-S	5.9 M	1.22 G	105.0	79.7
EfficientViT-B1 [r224]	9.1 M	0.52 G	73.0	79.4
ToMe-EfficientViT-B1 [r224]	9.1 M	0.47 G	73.0	78.8
ToFu-EfficientViT-B1 [r224]	9.1 M	0.47 G	73.0	79.0
LTMP-EfficientViT-B1 [r224]	9.1 M	0.50 G	73.3	79.2
LTM-EfficientViT-B1 [r224]	9.5 M	0.44 G	91.0	80.2
EfficientViT-B1 [r288]	9.1 M	0.86 G	95.5	80.4
ToMe-EfficientViT-B1 [r288]	9.1 M	0.73 G	95.5	79.7
ToFu-EfficientViT-B1 [r288]	9.1 M	0.73 G	95.5	89.8
LTMP-EfficientViT-B1 [r288]	9.1 M	0.76 G	95.9	80.0
LTM-EfficientViT-B1 [r288]	9.5 M	0.70 G	110.5	81.0

TABLE 6: Training time (minutes/epoch) comparisons between LTM-Transformers and their baseline models.

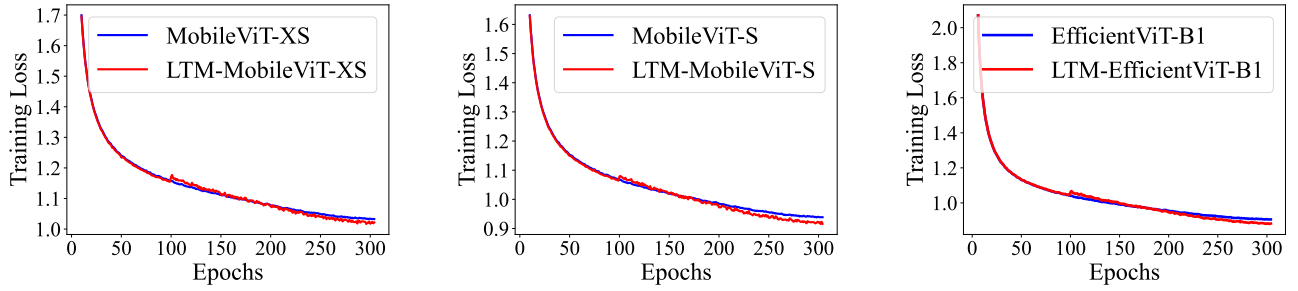
for both MobileViT-S and LTM-MobileViT-S across different transformer layers are illustrated in Figure 3. Both models contain 9 transformer layers. It is observed from Figure 3 that both $IB(G)$ and $IBB(G)$ decrease in deeper layers with larger layer indices of MobileViT-S and LTM-MobileViT-S. This observation suggests that features in deeper layers correlate more closely with the class labels and less with the input features, adhering to the IB principle. Moreover, LTM-MobileViT-S reduces both $IB(G)$ and $IBB(G)$ to lower levels in deeper layers compared to MobileViT-S. These observations evidence that the mask module in the LTM-Transformer block which generates the informative token merging task by (3) can effectively reduce both $IB(G)$ and $IBB(G)$, better adhering to the IB principle than the vanilla MobileViT-S. At the early stage of the training after 100 epochs, the IB bound and the IB loss of LTM-MobileViT-S are similar to those of the MobileViT-S. After training for 300 epochs, the IB bound and the IB loss of LTM-MobileViT-S are much smaller than those of the MobileViT-S.

5 MORE ABLATION STUDIES

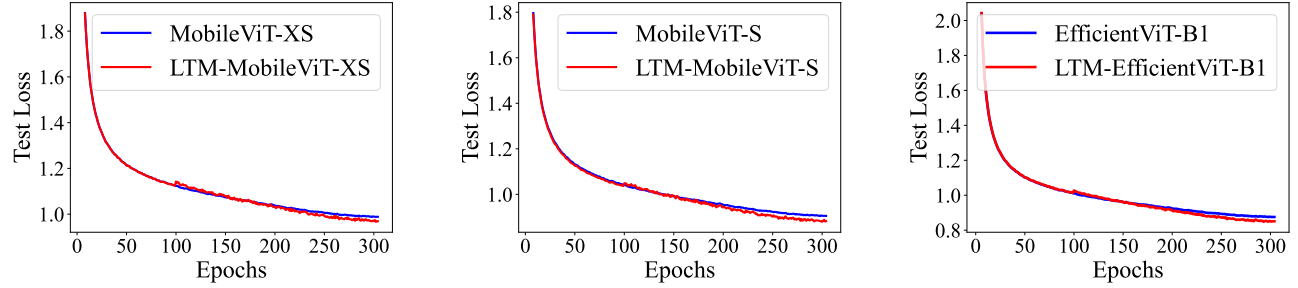
We conduct more ablation studies in this section, including the training time comparison, the training loss and test loss of LTM-Transformers, and the visualization results illustrating the effectiveness of a LTM-Transformer in selecting informative tokens during the token merging process. We compare the training time of LTM-Transformer models with the competing baselines for token merging in Table 6 in Section 5.1. Figure 4 in Section 5.2 illustrates the training loss and the test loss during the training process of LTM-Transformers and their baselines, highlighting that the test loss of the LTM-Transformer networks exhibits a more rapid decline compared to that of their baselines.

5.1 Training Time Evaluation

We evaluate the training cost of our LTM-Transformer models and the baseline models on the training set of ImageNet-1k. The training is performed on 4 NVIDIA A100 GPUs with an effective batch size of 512 images. We report the



(a) Training loss comparison between MobileViT-XS and LTM-MobileViT-XS. (b) Training loss comparison between MobileViT-S and LTM-MobileViT-S. (c) Training loss comparison between EfficientViT-B1 and LTM-EfficientViT-B1.



(d) Test loss comparison between MobileViT-XS and LTM-MobileViT-XS. (e) Test loss comparison between MobileViT-S and LTM-MobileViT-S. (f) Test loss comparison between EfficientViT-B1 and LTM-EfficientViT-B1.

Fig. 4: Training loss and test loss comparison between LTM-Transformer networks and corresponding baseline models.

overall training time of 300 epochs. We also include the training time of ToMe [14], ToFu [12], and LTMP [13] for comparison. It is noted that ToMe, ToFu, and LTMP are applied to pre-trained models. Therefore, the training time for ToMe, ToFu, and LTMP includes the training time of the baseline models. In contrast, our models are trained from scratch. The training time of various models are shown in Table 6. The training overhead of LTM-Transformers mainly comes from the computation of $\{\phi(\tilde{X}_i, a)\}_{i \in \mathcal{B}_j, a \in [C]}$, $\{Q^{(t-1)}(\tilde{X} \in a | Y = y)\}_{a \in [C], y \in [C]}$, and $\{\tilde{c}_a^{(t-1)}\}_{a=1}^C$ as described in Algorithm 1. It is observed from the Table 6 that the training time of LTM models is comparable to the training time of the competing token merging methods. In addition, LTM largely resolves the issue of significant prediction accuracy drops after token merging by ToMe, ToFu, and LTMP.

5.2 Training Loss and Test Loss of LTM-Transformers

In this section, we illustrate the training loss and the test loss of LTM-MobileViT-XS, LTM-MobileViT-S, and LTM-EfficientViT-B1. In comparison, we also illustrate the training loss and test loss of MobileViT-XS, MobileViT-S, and EfficientViT-B1. All the models are trained for 300 epochs. The plots are illustrated in Figure 4. It can be observed that LTM-Transformer networks achieve lower training losses and test losses at the end of the training, which demonstrates the benefit of LTM-Transformers in improving the performance of the visual transformers through the IB-inspired token merging.

5.3 Visualization Results

To study the effectiveness of LTM-Transformer in selecting informative tokens during the token merging process, we visualize the token merging masks in the first LTM-Transformer block of LTM-MobileViT-S for selected images from ImageNet in Figure 5. Each image is divided into 16×16 tokens. For each example, we select only the most representative merged token that encapsulates the critical features of the objects in the image, and the merged token is a weighted average of several self-attention output tokens with the aggregation weights in the token merging mask. The input images are illustrated in the first row, and the heatmaps that visualize the aggregation weights in the token merging mask for the selected merged token are shown in the second row. The class labels for each image are presented at the bottom of each column. The results illustrate that the mask module in the LTM-Transformer block usually assigns higher aggregation weights to tokens covering the most representative and distinctive parts of the objects, which are often the most informative for classifying the images. In the example of the dhole in the first column, the LTM-Transformer block puts larger weights on the eyes and nose of the dhole. In the example of the hartebeest in the second column, the LTM-Transformer block puts larger weights on the twisted horns of the hartebeest. In the example of the racing car in the third column, the LTM-Transformer block puts larger weights on the wheel of the car. In the example of the Stethoscope in the fourth column, the LTM-Transformer block puts larger weights on the diaphragm of the stethoscope. These observations demonstrate that more informative tokens contribute more to the merged tokens



Fig. 5: Visualization of merging weights in the first LTM-Transformer block in LTM-MobileViT-S.

with larger aggregation weights in the token merging process of the LTM-Transformer block.

6 PROOFS

6.1 Proof of Proposition 3.2

Proof. We first compute the gradient of $\phi(\tilde{X}_i(G), a')$ with respect to $\tilde{X}_i(G)$ by

$$\nabla_{\tilde{X}_i(G)} \phi(\tilde{X}_i(G), a') = \frac{2S_{ia'} \sum_{a=1}^C S_{ia} (\tilde{X}_i(G) - \tilde{c}_a) - 2S_{ia'} (\tilde{X}_i(G) - \tilde{c}_{a'}) \sum_{a=1}^C S_{ia}}{\left(\sum_{a=1}^C S_{ia}\right)^2}.$$

Using the definitions of γ_i and ζ_i as $\gamma_i := \sum_{a=1}^C S_{ia}$ and

$\zeta_i := \sum_{a=1}^C S_{ia} \tilde{c}_a$ for $i \in [n]$, we have

$$\nabla_{\tilde{X}_i(G)} \phi(\tilde{X}_i(G), a') = \frac{2S_{ia'}}{\gamma_i^2} (\gamma_i \tilde{c}_{a'} - \zeta_i).$$

As a result, the gradient of $\text{IBB}(G)$ with respect to G is computed as follows:

$$\begin{aligned} \nabla_G \text{IBB}(G) &= \frac{1}{n} \sum_{i=1}^n \sum_{a=1}^C \sum_{b=1}^C Z_i \nabla_{\tilde{X}_i} \phi(\tilde{X}_i, a) \phi(X_i, b) \log \phi(X_i, b) \\ &\quad - \frac{1}{n} \sum_{i=1}^n \sum_{a=1}^C \sum_{y=1}^C Z_i \nabla_{\tilde{X}_i} \phi(\tilde{X}_i, a) \mathbb{I}_{\{y_i=y\}} \log Q(\tilde{X} \in a | Y = y) \\ &= \frac{1}{n} \sum_{i=1}^n \sum_{a=1}^C Z_i \nabla_{\tilde{X}_i} \phi(\tilde{X}_i, a) \psi_{i,a} \\ &= \frac{2}{n} \sum_{i=1}^n \sum_{a=1}^C Z_i \frac{S_{ia}}{\gamma_i^2} (\gamma_i \tilde{c}_a - \zeta_i) \psi_{i,a}, \end{aligned}$$

where $\psi_{i,a} := \sum_{b=1}^C \phi(X_i, b) \log \phi(X_i, b) - \sum_{y=1}^C \mathbb{I}_{\{y_i=y\}} \log Q(\tilde{X} \in a | Y = y)$. \square

6.2 Proof of Theorem 3.1

We need the following two lemmas before the proof of Theorem 3.1. It is noted that we abbreviate $\tilde{X}(G)$ and $\tilde{X}_i(G)$ as \tilde{X} and \tilde{X}_i in the sequel.

Lemma 6.1.

$$\begin{aligned} I(\tilde{X}, X) &\leq \frac{1}{n} \sum_{i=1}^n \sum_{a=1}^C \sum_{b=1}^C \phi(\tilde{X}_i, a) \phi(X_i, b) \log \phi(X_i, b) \\ &\quad - \frac{1}{n^2} \sum_{i=1}^n \sum_{j=1}^n \sum_{b=1}^C \phi(X_i, b) \log \phi(X_j, b) \end{aligned} \quad (4)$$

Lemma 6.2.

$$I(\tilde{X}, Y) \geq \frac{1}{n} \sum_{a=1}^C \sum_{y=1}^C \sum_{i=1}^n \phi(\tilde{X}_i, a) \mathbb{I}_{\{y_i=y\}} \log Q(\tilde{X} \in a | Y = y) \quad (5)$$

Proof of Theorem 3.1. We note that $\text{IB}(\mathcal{W}) = I(\tilde{X}, X) - I(\tilde{X}, Y)$. Then $\text{IB}(\mathcal{W}) \leq \text{IBB}(\mathcal{W}) - C_0$ follows by the upper bound for $I(\tilde{X}, X)$ in Lemma 6.1 and the lower bound for $I(\tilde{X}, Y)$ in Lemma 6.2. Here $C_0 = \frac{1}{n^2} \sum_{i=1}^n \sum_{j=1}^n \sum_{b=1}^C \phi(X_i, b) \log \phi(X_j, b)$. \square

Proof of Lemma 6.1. By the log sum inequality, we have

$$\begin{aligned} I(\tilde{X}, X) &= \sum_{a=1}^C \sum_{b=1}^C \Pr[\tilde{X} \in a, X \in b] \log \frac{\Pr[\tilde{X} \in a, X \in b]}{\Pr[\tilde{X} \in a] \Pr[X \in b]} \\ &\leq \frac{1}{n^2} \sum_{i=1}^n \sum_{j=1}^n \sum_{a=1}^C \sum_{b=1}^C \phi(\tilde{X}_i, a) \phi(X_i, b) \left(\log \left(\phi(\tilde{X}_i, a) \phi(X_i, b) \right) \right. \\ &\quad \left. - \log \left(\phi(\tilde{X}_i, a) \phi(X_j, b) \right) \right) \\ &= \frac{1}{n^2} \sum_{i=1}^n \sum_{j=1}^n \sum_{a=1}^C \sum_{b=1}^C \phi(\tilde{X}_i, a) \phi(X_i, b) \log \phi(X_i, b) \\ &\quad - \frac{1}{n^2} \sum_{i=1}^n \sum_{j=1}^n \sum_{a=1}^C \sum_{b=1}^C \phi(\tilde{X}_i, a) \phi(X_i, b) \log \phi(X_j, b) \\ &= \frac{1}{n} \sum_{i=1}^n \sum_{a=1}^C \sum_{b=1}^C \phi(\tilde{X}_i, a) \phi(X_i, b) \log \phi(X_i, b) \end{aligned}$$

$$- \frac{1}{n^2} \sum_{i=1}^n \sum_{j=1}^n \sum_{a=1}^C \sum_{b=1}^C \phi(\tilde{X}_i, a) \phi(X_i, b) \log \phi(X_j, b). \quad (6)$$

□

Proof of Lemma 6.2. Let $Q(\tilde{X}|Y)$ be a variational distribution. We have

$$\begin{aligned} & I(\tilde{X}, Y) \\ &= \sum_{a=1}^C \sum_{y=1}^C \Pr[\tilde{X} \in a, Y = y] \log \frac{\Pr[\tilde{X} \in a, Y = y]}{\Pr[\tilde{X} \in a] \Pr[Y = y]} \\ &= \sum_{a=1}^C \sum_{y=1}^C \Pr[\tilde{X} \in a, Y = y] \log \frac{\Pr[\tilde{X} \in a|Y = y] Q(\tilde{X} \in a|Y = y)}{\Pr[\tilde{X} \in a] Q(\tilde{X} \in a|Y = y)} \\ &\geq \sum_{a=1}^C \sum_{y=1}^C \Pr[\tilde{X} \in a, Y = y] \log \frac{\Pr[\tilde{X} \in a|Y = y]}{Q(\tilde{X} \in a|Y = y)} \\ &+ \sum_{a=1}^C \sum_{y=1}^C \Pr[\tilde{X} \in a, Y = y] \log \frac{Q(\tilde{X} \in a|Y = y)}{\Pr[\tilde{X} \in a]} \\ &= \text{KL}(P(\tilde{X}|Y) \| Q(\tilde{X}|Y)) \\ &+ \sum_{a=1}^C \sum_{y=1}^C \Pr[\tilde{X} \in a, Y = y] \log \frac{Q(\tilde{X} \in a|Y = y)}{\Pr[\tilde{X} \in a]} \\ &\geq \sum_{a=1}^C \sum_{y=1}^C \Pr[\tilde{X} \in a, Y = y] \log \frac{Q(\tilde{X} \in a|Y = y)}{\Pr[\tilde{X} \in a]} \\ &= \sum_{a=1}^C \sum_{y=1}^C \Pr[\tilde{X} \in a, Y = y] \log Q(\tilde{X} \in a|Y = y) + H(P(\tilde{X})) \\ &\geq \sum_{a=1}^C \sum_{y=1}^C \Pr[\tilde{X} \in a, Y = y] \log Q(\tilde{X} \in a|Y = y) \\ &\geq \frac{1}{n} \sum_{a=1}^C \sum_{y=1}^C \sum_{i=1}^n \phi(\tilde{X}_i, a) \mathbb{I}_{\{y_i=y\}} \log Q(\tilde{X} \in a|Y = y). \quad (7) \end{aligned}$$

□

6.3 Computation of $Q^{(t)}(\tilde{\mathbf{X}}|Y)$

The variational distribution $Q^{(t)}(\tilde{\mathbf{X}}|Y)$ can be computed by

$$\begin{aligned} Q^{(t)}(\tilde{X} \in a|Y = y) &= \Pr[\tilde{X} \in a|Y = y] \\ &= \frac{\sum_{i=1}^n \phi(\tilde{X}_i, a) \mathbb{I}_{\{y_i=y\}}}{\sum_{i=1}^n \mathbb{I}_{\{y_i=y\}}}. \quad (8) \end{aligned}$$

7 CONCLUSION

In this paper, we propose a novel transformer block, Transformer with Learnable Token Merging, or LTM-Transformer. LTM-Transformer blocks perform token merging so as to render a transformer network with less FLOPs and faster inference speed. A LTM-Transformer block generates an informative token merging mask for token merging in a learnable manner, which is inspired by the reduction of the Information-Bottleneck loss. A network with LTM-Transformer blocks can be trained with standard SGD, and it enjoys a reduction of IB loss and reduced FLOPs while maintaining a compelling prediction accuracy. We demonstrate the effectiveness of LTM-Transformer by replacing all the transformer blocks in several popular visual transformers with LTM-Transformer blocks. Extensive experiments on various tasks demonstrate the effectiveness of LTM-Transformer.

REFERENCES

- [1] A. Vaswani, N. Shazeer, N. Parmar, J. Uszkoreit, L. Jones, A. N. Gomez, Ł. Kaiser, and I. Polosukhin, "Attention is all you need," in *Advances in neural information processing systems*, 2017, pp. 5998–6008.
- [2] L. Yuan, Y. Chen, T. Wang, W. Yu, Y. Shi, Z. Jiang, F. E. Tay, J. Feng, and S. Yan, "Tokens-to-token vit: Training vision transformers from scratch on imagenet," in *Proceedings of the IEEE/CVF international conference on computer vision*, 2021.
- [3] A. Dosovitskiy, L. Beyer, A. Kolesnikov, D. Weissenborn, X. Zhai, T. Unterthiner, M. Dehghani, M. Minderer, G. Heigold, S. Gelly, J. Uszkoreit, and N. Houlsby, "An image is worth 16x16 words: Transformers for image recognition at scale," in *International Conference on Learning Representations*, 2021.
- [4] Z. Liu, Y. Lin, Y. Cao, H. Hu, Y. Wei, Z. Zhang, S. Lin, and B. Guo, "Swin transformer: Hierarchical vision transformer using shifted windows," *arXiv preprint arXiv:2103.14030*, 2021.
- [5] X. Zhu, W. Su, L. Lu, B. Li, X. Wang, and J. Dai, "Deformable detr: Deformable transformers for end-to-end object detection," *ICLR*, 2021.
- [6] J. Liang, J. Cao, G. Sun, K. Zhang, L. Van Gool, and R. Timofte, "Swinir: Image restoration using swin transformer," *ICCV*, 2021.
- [7] H. Cai, C. Gan, and S. Han, "Efficientvit: Enhanced linear attention for high-resolution low-computation visual recognition," in *Proceedings of the IEEE/CVF International Conference on Computer Vision*, 2023.
- [8] H. Touvron, M. Cord, M. Douze, F. Massa, A. Sablayrolles, and H. Jégou, "Training data-efficient image transformers & distillation through attention," in *International conference on machine learning*. PMLR, 2021.
- [9] S. Han, J. Pool, J. Tran, and W. Dally, "Learning both weights and connections for efficient neural network," in *Advances in Neural Information Processing Systems*, 2015, pp. 1135–1143.
- [10] Z. Zhou, H. Yao, X. Guo, and Y. Xu, "Rethinking the value of network pruning," in *Proceedings of the IEEE/CVF Conference on Computer Vision and Pattern Recognition*, 2020, pp. 5867–5875.
- [11] W. Sun, Y. Jiang, S. Zhang, and Y. Liu, "Cascade pruning: Towards class imbalance in convolutional neural networks," in *Proceedings of the IEEE/CVF Conference on Computer Vision and Pattern Recognition*, 2021, pp. 9860–9869.
- [12] M. Kim, S. Gao, Y.-C. Hsu, Y. Shen, and H. Jin, "Token fusion: Bridging the gap between token pruning and token merging," in *Proceedings of the IEEE/CVF Winter Conference on Applications of Computer Vision*, 2024, pp. 1383–1392.
- [13] M. Bonnaerens and J. Dambre, "Learned thresholds token merging and pruning for vision transformers," *Transactions on Machine Learning Research*, 2023.
- [14] D. Bolya, C.-Y. Fu, X. Dai, P. Zhang, C. Feichtenhofer, and J. Hoffman, "Token merging: Your vit but faster," *ICLR*, 2023.
- [15] Y. Rao, W. Zhao, B. Liu, J. Lu, J. Zhou, and C.-J. Hsieh, "Dynamicvit: Efficient vision transformers with dynamic token sparsification," *arXiv preprint arXiv:2106.02034*, 2021.
- [16] I. Bello, B. Zoph, A. Vaswani, J. Shlens, and Q. V. Le, "Attention augmented convolutional networks," in *Proceedings of the IEEE/CVF international conference on computer vision*, 2019, pp. 3286–3295.
- [17] S. Mehta and M. Rastegari, "Mobilevit: light-weight, general-purpose, and mobile-friendly vision transformer," *ICLR*, 2022.
- [18] A. Dosovitskiy, L. Beyer, A. Kolesnikov, D. Weissenborn, X. Zhai, T. Unterthiner, M. Dehghani, M. Minderer, G. Heigold, S. Gelly, J. Uszkoreit, and N. Houlsby, "An image is worth 16x16 words: Transformers for image recognition at scale," in *ICLR*, 2021.
- [19] N. Carion, F. Massa, G. Synnaeve, N. Usunier, A. Kirillov, and S. Zagoruyko, "End-to-end object detection with transformers," in *Computer Vision—ECCV 2020: 16th European Conference, Glasgow, UK, August 23–28, 2020, Proceedings, Part I 16*. Springer, 2020.
- [20] Y. Wang, N. Xu, C. Chen, and Y. Yang, "Adaptive cross-layer attention for image restoration," *arXiv preprint arXiv:2203.03619*, 2022.
- [21] X. Liu, H. Peng, N. Zheng, Y. Yang, H. Hu, and Y. Yuan, "Efficientvit: Memory efficient vision transformer with cascaded group attention," in *Proceedings of the IEEE/CVF Conference on Computer Vision and Pattern Recognition*, 2023, pp. 14 420–14 430.
- [22] B. Graham, A. El-Nouby, H. Touvron, P. Stock, A. Joulin, H. Jégou, and M. Douze, "Levit: a vision transformer in convnet's clothing for faster inference," in *Proceedings of the IEEE/CVF international conference on computer vision*, 2021, pp. 12 259–12 269.

- [23] I. Radosavovic, R. P. Kosaraju, R. Girshick, K. He, and P. Dollár, "Designing network design spaces," in *Proceedings of the IEEE/CVF conference on computer vision and pattern recognition*, 2020.
- [24] C. Gong, D. Wang, M. Li, X. Chen, Z. Yan, Y. Tian, Qiang Liu, and V. Chandra, "NASvit: Neural architecture search for efficient vision transformers with gradient conflict aware supernet training," in *International Conference on Learning Representations*, 2022.
- [25] T. Chen, Y. Cheng, Z. Gan, L. Yuan, L. Zhang, and Z. Wang, "Chasing sparsity in vision transformers: An end-to-end exploration," *Advances in Neural Information Processing Systems*, 2021.
- [26] F. Yu, K. Huang, M. Wang, Y. Cheng, W. Chu, and L. Cui, "Width & depth pruning for vision transformers," in *Proceedings of the AAAI Conference on Artificial Intelligence*, vol. 36, no. 3, 2022, pp. 3143–3151.
- [27] Z. Kong, P. Dong, X. Ma, X. Meng, W. Niu, M. Sun, X. Shen, G. Yuan, B. Ren, H. Tang *et al.*, "Spvit: Enabling faster vision transformers via latency-aware soft token pruning," in *Computer Vision—ECCV 2022: 17th European Conference, Tel Aviv, Israel, October 23–27, 2022, Proceedings, Part XI*. Springer, 2022, pp. 620–640.
- [28] A. Chavan, Z. Shen, Z. Liu, Z. Liu, K.-T. Cheng, and E. P. Xing, "Vision transformer slimming: Multi-dimension searching in continuous optimization space," in *Proceedings of the IEEE/CVF Conference on Computer Vision and Pattern Recognition*, 2022, pp. 4931–4941.
- [29] C. Zheng, K. Zhang, Z. Yang, W. Tan, J. Xiao, Y. Ren, S. Pu *et al.*, "Savit: Structure-aware vision transformer pruning via collaborative optimization," *Advances in Neural Information Processing Systems*, vol. 35, pp. 9010–9023, 2022.
- [30] S. Yu, T. Chen, J. Shen, H. Yuan, J. Tan, S. Yang, J. Liu, and Z. Wang, "Unified visual transformer compression," *ICLR*, 2022.
- [31] Z. Wang, H. Luo, P. Wang, F. Ding, F. Wang, and H. Li, "Vtc-lfc: Vision transformer compression with low-frequency components," *Advances in Neural Information Processing Systems*, vol. 35, 2022.
- [32] A. M. Saxe, Y. Bansal, J. Dapello, M. Advani, A. Kolchinsky, B. D. Tracey, and D. D. Cox, "On the information bottleneck theory of deep learning," *Journal of Statistical Mechanics: Theory and Experiment*, vol. 2019, no. 12, p. 124020, 2019.
- [33] Q. Lai, Y. Li, A. Zeng, M. Liu, H. Sun, and Q. Xu, "Information bottleneck approach to spatial attention learning," in *Proceedings of the Thirtieth International Joint Conference on Artificial Intelligence, IJCAI 2021, Virtual Event / Montreal, Canada, 19-27 August 2021*, Z. Zhou, Ed. ijcai.org, 2021, pp. 779–785.
- [34] D. Zhou, Z. Yu, E. Xie, C. Xiao, A. Anandkumar, J. Feng, and J. M. Alvarez, "Understanding the robustness in vision transformers," in *International Conference on Machine Learning*. PMLR, 2022, pp. 27378–27394.
- [35] A. Dosovitskiy, L. Beyer, A. Kolesnikov, D. Weissenborn, X. Zhai, T. Unterthiner, M. Dehghani, M. Minderer, G. Heigold, S. Gelly, J. Uszkoreit, and N. Houlsby, "An image is worth 16x16 words: Transformers for image recognition at scale," in *9th International Conference on Learning Representations, ICLR 2021, Virtual Event, Austria, May 3-7, 2021*. OpenReview.net, 2021.
- [36] O. Russakovsky, J. Deng, H. Su, J. Krause, S. Satheesh, S. Ma, Z. Huang, A. Karpathy, A. Khosla, M. Bernstein *et al.*, "Imagenet large scale visual recognition challenge," *International journal of computer vision*, vol. 115, no. 3, pp. 211–252, 2015.
- [37] Y. Li, G. Yuan, Y. Wen, J. Hu, G. Evangelidis, S. Tulyakov, Y. Wang, and J. Ren, "Efficientformer: Vision transformers at mobilenet speed," *Advances in Neural Information Processing Systems*, vol. 35, pp. 12934–12949, 2022.
- [38] T. Chen, Y. Cheng, Z. Gan, L. Yuan, L. Zhang, and Z. Wang, "Chasing sparsity in vision transformers: An end-to-end exploration," *Advances in Neural Information Processing Systems*, vol. 34, 2021.
- [39] Z. Kong, P. Dong, X. Ma, X. Meng, W. Niu, M. Sun, X. Shen, G. Yuan, B. Ren, H. Tang *et al.*, "Spvit: Enabling faster vision transformers via latency-aware soft token pruning," in *European Conference on Computer Vision*. Springer, 2022, pp. 620–640.
- [40] C. Zheng, K. Zhang, Z. Yang, W. Tan, J. Xiao, Y. Ren, S. Pu *et al.*, "Savit: Structure-aware vision transformer pruning via collaborative optimization," *Advances in Neural Information Processing Systems*, vol. 35, pp. 9010–9023, 2022.
- [41] M. Sandler, A. Howard, M. Zhu, A. Zhmoginov, and L.-C. Chen, "Mobilenetv2: Inverted residuals and linear bottlenecks," in *Proceedings of the IEEE conference on computer vision and pattern recognition*, 2018, pp. 4510–4520.
- [42] T.-Y. Lin, M. Maire, S. Belongie, J. Hays, P. Perona, D. Ramanan, P. Dollár, and C. L. Zitnick, "Microsoft coco: Common objects in context," in *European conference on computer vision*. Springer, 2014.
- [43] A. Howard, M. Sandler, G. Chu, L.-C. Chen, B. Chen, M. Tan, W. Wang, Y. Zhu, R. Pang, V. Vasudevan *et al.*, "Searching for mobilenetv3," in *Proceedings of the IEEE/CVF International Conference on Computer Vision*, 2019, pp. 1314–1324.
- [44] A. G. Howard, M. Zhu, B. Chen, D. Kalenichenko, W. Wang, T. Weyand, M. Andreetto, and H. Adam, "Mobilenets: Efficient convolutional neural networks for mobile vision applications," *arXiv preprint arXiv:1704.04861*, 2017.
- [45] M. Tan and Q. V. Le, "Mixconv: Mixed depthwise convolutional kernels," in *Proceedings of the British Machine Vision Conference (BMVC)*, 2019.
- [46] M. Tan, B. Chen, R. Pang, V. Vasudevan, M. Sandler, A. Howard, and Q. V. Le, "Mnasnet: Platform-aware neural architecture search for mobile," in *Proceedings of the IEEE/CVF Conference on Computer Vision and Pattern Recognition*, 2019, pp. 2820–2828.
- [47] J. Redmon and A. Farhadi, "Yolo9000: better, faster, stronger," in *Proceedings of the IEEE conference on computer vision and pattern recognition*, 2017, pp. 7263–7271.
- [48] H. Song, D. Sun, S. Chun, V. Jampani, D. Han, B. Heo, W. Kim, and M.-H. Yang, "VidT: An efficient and effective fully transformer-based object detector," *ICLR*, 2022.
- [49] K. He, G. Gkioxari, P. Dollár, and R. Girshick, "Mask r-cnn," in *Proceedings of the IEEE international conference on computer vision*, 2017, pp. 2961–2969.
- [50] K. Chen, J. Wang, J. Pang, Y. Cao, Y. Xiong, X. Li, S. Sun, W. Feng, Z. Liu, J. Xu *et al.*, "Mmdetection: Open mmlab detection toolbox and benchmark," *arXiv preprint arXiv:1906.07155*, 2019.